

# A hybrid microfluidic system for regulation of neural differentiation in induced pluripotent stem cells

Zahra Hesari,<sup>1,2</sup> Massoud Soleimani,<sup>3</sup> Fatemeh Atyabi,<sup>1,2</sup> Meysam Sharifdini,<sup>4</sup> Samad Nadri,<sup>5</sup> Majid Ebrahimi Warkiani,<sup>6</sup> Mehrak Zare,<sup>7</sup> Rassoul Dinarvand<sup>1,2</sup>

<sup>1</sup>Department of Pharmaceutics, Faculty of Pharmacy, Tehran University of Medical Sciences, Tehran, Iran

<sup>2</sup>Nanotechnology Research Centre, Faculty of Pharmacy, Tehran University of Medical Sciences, Tehran, Iran

<sup>3</sup>Department of Hematology and Blood Banking, Faculty of Medicine, Tarbiat Modares University, Tehran, Iran

<sup>4</sup>Department of Medical Microbiology, School of Medicine, Guilan University of Medical Sciences, Rasht, Iran

<sup>5</sup>Medical Biotechnology and Nanotechnology Department, Faculty of Medicine, Zanjan University of Medical Science, Zanjan, Iran

<sup>6</sup>School of Mechanical and Manufacturing Engineering, Australian Centre for NanoMedicine, University of New South Wales, Sydney, Australia

<sup>7</sup>Skin and Stemcell Research Center, Tehran University of Medical Sciences, Tehran, Iran

Received 13 January 2016; accepted 16 February 2016

Published online 11 March 2016 in Wiley Online Library (wileyonlinelibrary.com). DOI: 10.1002/jbm.a.35689

**Abstract:** Controlling cellular orientation, proliferation, and differentiation is valuable in designing organ replacements and directing tissue regeneration. In the present study, we developed a hybrid microfluidic system to produce a dynamic microenvironment by placing aligned PDMS microgrooves on surface of biodegradable polymers as physical guidance cues for controlling the neural differentiation of human induced pluripotent stem cells (hiPSCs). The neuronal differentiation capacity of cultured hiPSCs in the microfluidic system and other control groups was investigated using quantitative real time PCR (qPCR) and immunocytochemistry. The functionality of differentiated hiPSCs inside hybrid system's scaffolds was also evaluated on the rat hemisectioned spinal cord in acute phase. Implanted cell's fate was examined using tissue freeze section and the functional recovery was evaluated according to the Basso, Beattie, and Bresnahan (BBB) locomotor rating scale. Our results confirmed the dif-

ferentiation of hiPSCs to neuronal cells on the microfluidic device where the expression of neuronal-specific genes was significantly higher compared to those cultured on the other systems such as plain tissue culture dishes and scaffolds without fluidic channels. Although survival and integration of implanted hiPSCs did not lead to a significant functional recovery, we believe that combination of fluidic channels with nanofiber scaffolds provides a great microenvironment for neural tissue engineering, and can be used as a powerful tool for *in situ* monitoring of differentiation potential of various kinds of stem cells. © 2016 Wiley Periodicals, Inc. *J Biomed Mater Res Part A*: 104A: 1534–1543, 2016.

**Key Words:** microfluidics, human induced pluripotent stem cells (hiPSCs), neural differentiation, tissue engineering, nanofibers

**How to cite this article:** Hesari Z, Soleimani M, Atyabi F, Sharifdini M, Nadri S, Warkiani ME, Dinarvand R. 2016. A hybrid microfluidic system for regulation of neural differentiation in induced pluripotent stem cells. *J Biomed Mater Res Part A* 2016;104A:1534–1543.

## INTRODUCTION

Spinal cord injuries can be devastating, resulting in paralysis, loss of sensation, and ultimately permanent disability. Absence of movement and sensation occurs in spinal cord injury (SCI) below the level of the injured spinal cord. To date, no efficient treatment has taken place to completely repair SCI.<sup>1,2</sup> Recently, transplantation of stem and progenitor cells incorporating various types of scaffolds to the injury sites has shown auspicious results for SCI therapy.<sup>1,3</sup>

Stem cells play a pivotal role in the human body for tissue regeneration and they are now used as an integral part of modern clinical treatment.<sup>4</sup> Over the past decades, numerous attempts are devoted toward neural differentia-

tion of stem cells.<sup>5</sup> Various sources of stem cells such as neural stem cells (NSCs) or neural progenitor cells (NPCs) have been studied for treatment of SCI and varying levels of improvement in animal models have been demonstrated.<sup>3,6</sup> However, the clinical utility of these cells is hampered with problems such as limited growth yield and lack of proper functionality.<sup>7</sup> Therefore, alternative sources of adult stem cells have attracted great interest for treatment of neurodegenerative disorders.<sup>8</sup>

It has been discovered that human induced pluripotent stem cells (hiPSCs) which are achieved by activating a combination of a limited number of reprogramming genes, can be differentiated into neural cells.<sup>9–11</sup> Because of their

Additional Supporting Information may be found in the online version of this article.

**Correspondence to:** R. Dinarvand; e-mail: dinarvand@tums.ac.ir

production from somatic cells no ethical obstacles are encountered when using hiPSCs. Moreover, hiPSCs have the potential of self-renewal and differentiation into a broad range of cell types, providing a limitless, invaluable and promising source of pluripotent stem cells for cellular therapy.<sup>12,13</sup> The wide area of the therapeutic potential of the hiPSCs is explained in different principle diseases.<sup>14–17</sup> Additionally, value of these cells for treatment of some neurodevelopmental disorders such as Parkinson's,<sup>18</sup> Huntington's,<sup>19</sup> multiple sclerosis<sup>20</sup> and spinal cord injury<sup>21</sup> has been also demonstrated.

Molecular biologists usually employ chemical factors to induce differentiation of stem cells into specific lineage; however, guided differentiation of stem cells using these strategies is not efficient and often requires long term cell cultures.<sup>22</sup> This has limited the widespread use of stem cell therapy. Therefore, there is a need to develop efficient methods for enhancing hiPSCs differentiation by providing a stem cell niche.<sup>23</sup>

Recently, growing evidence suggests that matrix-mediated signals (i.e., extracellular matrix (ECM) microenvironment) such as strain, flow-induced shear stress, substrate rigidity and topography have a more profound impact on stem cell phenotypes than had previously been recognized.<sup>23–25</sup> Using a variety of cell culture models enabled by microfluidic systems, we are beginning to systematically investigate the dynamic response of stem cells to combinations of relevant mechanobiological stimuli in order to guide and enhance their differentiation.<sup>24,26</sup>

With the advent of microfluidics, many of the previous hurdles of *in vitro* testing were eliminated through greater control or combined functionalities, allowing one to create specific micro-environment with *in vivo*-like physiological topography.<sup>27,28</sup> In this work, we utilized the power of micro-engineering to develop a hybrid microfluidic system for *in vitro* differentiation of hiPSCs into neuronal cells. Our device comprised of a polymeric substrate made by electrospinning (i.e., three-dimensional scaffold to which they adhere) mimicking the condition of ECM and a fluidic network on top for applying physiologically relevant interstitial flow levels.<sup>29</sup> We hypothesize that this dynamic microenvironment emulates the key biomechanical interactions *in vivo*, thus enabling successful induction of hiPSCs into neural cells for tissue engineering. To our knowledge, the synergistic effects of multiple stimuli involving physical (topographical) cues in conjunction with chemical and biological cues on neural differentiation have not been explored before. Our preliminary results confirmed that microfluidic system could enhance and diminish the expression of some neuronal genes. Quantitative polymerase chain reaction (qPCR) analysis of differentiated cell inside the microfluidic system indicated that neural genes including  $\beta$ -tubulin III was expressed at higher levels while GFAP<sup>30</sup> genes were expressed at lower levels compared to cells differentiated on our control systems. Taken together, these results imply that hiPSCs differentiated on microfluidic devices are more likely to differentiate toward neural cells, while hiPSCs differentiated on poly(lactic-co-glycolic) acid (PLGA) scaffolds

and tissue culture dishes preferentially differentiate into glial cells. Figure 1(a) shows schematic representation of the assembled and separated parts of our microfluidic device for loading and differentiation of stem cells.

## MATERIALS AND METHODS

### Fabrication of microfluidic channels

Microfluidic channels were fabricated using soft lithography process described elsewhere.<sup>31</sup> To obtain microfluidic channels of 40- $\mu\text{m}$  height, SU8-50 was spin coated (MicroChem Corp.) on a silicon wafer at 3000 rpm for 30 s, then it was soft baked on a hot-plate at 65°C for 5 min and 95°C for 30 min until the solvent evaporated and the film was densified. After cooling down, SU8 resist was subjected to 360–440 nm UV radiation at 300 mJ cm<sup>-2</sup> through a mask with predefined patterns. Following exposure, the wafer was baked at 65°C and 95°C for 2 and 4 min, respectively. After cooling down the wafer to the room temperature, it was submerged inside the SU8 developer (Microposit EC solvent, Chestech) for development using manual agitation. The final master mold obtained by rinsing the wafer with isopropanol alcohol (IPA) followed by drying using the nitrogen gas. The surface of the wafer was also salinized using the trichloro (1,1,2,2-perfluoroethyl) silane in a desiccator for 40 min. To form the microfluidic device, Sylgard 184 (Dow Corning) was mixed in a 10:1 (w/w) ratio of resin to crosslinker, degassed and then casted on channel masters to form PDMS channels with a thickness of 2 mm. Cured PDMS channels were then peeled from the SU-8 master and access holes punched using a Harris Micro-Punch®.

### Fabrication of electrospun nanofibrous PLGA scaffolds

Nanofibrous PLGA scaffolds were fabricated using an in-house electrospinning technique. Briefly, a 12% solution of PLGA (75/25, Bohringer) and 0.08% of tetra ethyl ammonium bromide (TEAB) in chloroform: dimethylformamide (3:1) solvent system was emulsified with aqueous solution of BDNF and EGF neurotrophic factors with final concentration of 200 and 500 ng mL<sup>-1</sup> of emulsion, respectively. Emulsification was performed using 600 rpm centrifugation for 1 min. Aligned nanofibrous scaffolds were obtained using high speed (3000 rpm) rotating disk. Plain PLGA scaffold without neurotrophic factors was also fabricated with the aforementioned parameters. A low frequency plasma generator of 40 kHz frequency with a cylindrical quartz reactor (Diener Electronics, Germany) was used for surface modification of the nanofibers. Pure oxygen was introduced into the reaction chamber of the system at 0.4 mbar pressure and purged for 10–15 min before beginning the treatment; subsequently, the glow discharge was ignited for 5 min.

### ECM (fibronectin) grafting

Plasma treated sheets were immersed in 1-ethyl-3-(3-dimethylaminopropyl)carbodiimide/*N*-hydroxysuccinimide (Merck, Germany) solution (10 mg mL<sup>-1</sup>) overnight at 4°C and protected from exposure to the light. In the next step, scaffolds were immersed in 50  $\mu\text{g mL}^{-1}$  fibronectin solution

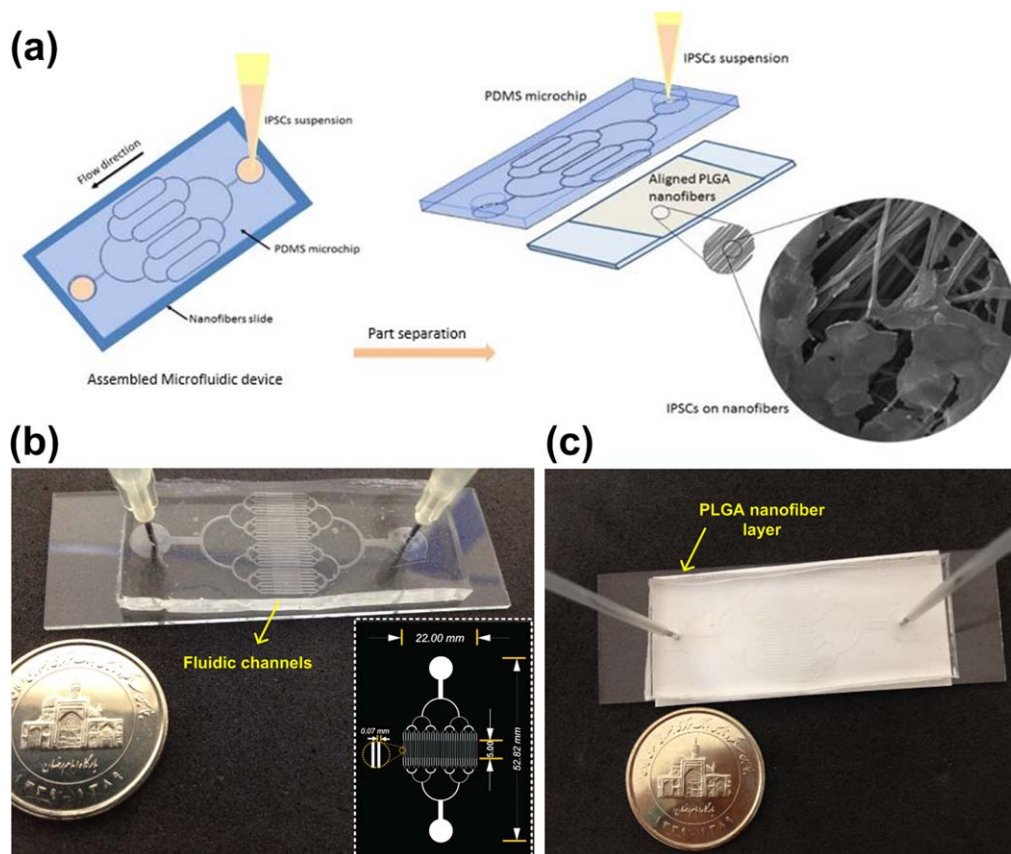


**FIGURE 1.** Hybrid microfluidic system construction. (a) Schematic representation of assembled and separated parts of hybrid device for stem cell loading and differentiation. (b) Optical image of the PDMS microchip with fluidic channels. The cells cultured in 32 identical microchambers were subjected to slow level of fluidic flows simultaneously. (c) Optical image of the hybrid device comprised of the PDMS chip on top and PLGA coated glass substrate at the bottom.

(Sigma–Aldrich, USA) overnight at 4°C to enhance cell attachment after seeding.

#### ATR-FTIR analysis

Surface chemical modifications after plasma treatment and fibronectin grafting were investigated by attenuated total reflection Fourier transform infrared (ATR-FTIR). The spectra were recorded using an Equinox 55 spectrometer (Bruker Optics) equipped with a deuterated triglycine sulfate (DTGS) detector and a diamond ATR crystal.

#### Scanning electron microscopy (SEM)

The cell–polymer constructs were fixed in 2.5% glutaraldehyde dehydrated through a graded series of ethanol, vacuum dried, mounted onto aluminum stubs, and sputter coated with gold. Samples were examined using a scanning electron microscope (KYKY EM-3200 and S-4500; Hitachi, Japan) at an accelerating voltage of 17–25 kV.

#### MTT assay

MTT assay was used to evaluate the proliferation of hiPSCs on PLGA nanofibers, plasma treated PLGA and fibronectin treated PLGA nanofibrous scaffolds. Sterilized nanofibrous membranes were placed in a 48-well culture plate, seeded at a cell density of  $4 \times 10^3$  cells per  $\text{cm}^2$  and incubated at

37°C, 5%  $\text{CO}_2$ . On days 1, 3, and 5 after cell seeding, 50  $\mu\text{L}$  MTT (3-(4,5-dimethyl-thiazolyl-2)-2,5-diphenoltetrazolium bromide) solution (5  $\text{mg mL}^{-1}$  in DMEM) was added to each well ( $n = 4$ ). The plate was incubated at 37°C for 3 h for conversion of MTT to formazan crystals by the mitochondrial dehydrogenases of living cells. For dissolution of the dark-blue intracellular formazan, the supernatant was removed and a constant amount of dimethyl sulfoxide solvent was added. The optical density was read at a wavelength of 570 nm in a micro-plate reader (BioTek Instruments, USA). The same procedure was performed for cultured cells in tissue culture polystyrene (TCPS) as a control.

#### Cell culture

The hiPSCs were obtained from the cell bank of Stem Cell Technology Research Center (Tehran, Iran) as described previously by our group.<sup>32</sup> These cells were cultured on mitotically (Invitrogen, USA) inactivated feeder layers of SNL76/7 cells in 6-cm Petri dishes (SPL Life Sciences, Korea), covered with 0.1% gelatin in PBS (both Invitrogen). The feeder cells were passaged every 3 days with DMEM culture medium supplemented with 10% FBS; every 5–6 days hiPSC colonies were detached with 0.1% collagenase IV (Invitrogen), and replaced onto inactivated SNL76/7 cells (utilizing

mitomycin). hiPSC medium containing DMEM/F12 culture medium supplemented with 10% FBS-ESC qualified, 0.1 mmol L<sup>-1</sup> nonessential amino acids, 1 mmol L<sup>-1</sup> L-glutamine, 20 ng mL<sup>-1</sup> basic fibroblast growth factor (bFGF) (all from Invitrogen) and penicillin (50 U mL<sup>-1</sup>)/streptomycin (50 µg mL<sup>-1</sup>) (all from Sigma-Aldrich, St. Louis, MO), and about 50% of the medium was replaced every day.

#### **In vitro differentiation of hiPSCs into neuronal lineages**

HiPSCs were pipetted and seeded into the channels of hybrid microfluidic chip and fabricated scaffold in DMEMF12/FBS (10%) media for 8 days. The cells were plated on tissue culture plastic polystyrene (TCPS) in neural induction media consisting of DMEMF12/FBS (10%), 20 ng mL<sup>-1</sup> BDNF and 50 ng mL<sup>-1</sup> EGF (Pepro Tech, USA) as a control. The hiPSCs colonies (seeded in device, scaffolds and TCPS) were incubated in 5% CO<sub>2</sub> at 37°C for 8 days. Supplemented culture medium was replaced every 24 h and the differentiated cells were examined for gene and protein expression.

#### **Quantitative real-time PCR**

The total cellular RNA was extracted using RNxPLus (CinnaGen, Iran) according to the manufacturer's protocol and random hexamer primed cDNA synthesis was carried out with Revert Aid first strand cDNA synthesis kit (Fermentas, Burlington, Canada). The cDNA was used for 40 cycle PCR in Rotor Gene 6000 (Corbett Research, Australia) with a total volume of 13 µL containing 6.25 µL of SYBR PCR Premix EX Taq<sup>TM</sup> (Perfect Real Time; Takara), 600 nM of final concentration for each primer, 1 µL template and sufficient distilled water to reach the volume of 13 µL. The cycling parameters for qPCR were as follows: 10 min at 95°C for initial denaturation, followed by forty cycles of 15 s at 95°C and 1 min at 60–62°C, and finally, melting of PCR products at 50–90°C to confirm PCR specificity by using melting curve analysis. All the samples were analyzed in duplicate, and the average values were used for quantification. The relative quantitative model was performed to calculate the expression of the target gene in comparison to β-actin as the endogenous control. Genes and the related specific primers are represented in Supporting Information Table SI.

#### **Immunocytochemistry analysis**

The cells were fixed with 4% paraformaldehyde (Sigma, USA) for 20 min and then permeabilized with 0.4% Triton X100 in PBS for 10 min. The fixed cells were blocked for 30 min at 37°C with 5% goat serum/PBS-tween-20 and were reacted overnight at 4°C with the respective primary antibodies of β-tubulin III (1:50 Chemicon) and NSE (1:100 Chemicon). At the end of the incubation time, the cells were rinsed three times with PBS-tween-20 (0.1%) and were incubated with the Fluorescein isothiocyanate (FITC)-conjugated anti mouse IgG as the secondary antibody (1:100 Sigma) at 37°C for 1 h. The nuclei were counterstained with DAPI (Sigma), and the cells were then analyzed with a fluorescent microscope (Nikon, Japan).

#### **Recombinant lentiviruses constructions**

About 24 h prior to transfection, 6–8 × 10<sup>6</sup> HEK293T cells were plated into 100-mm dishes in 10 mL of fresh DMEM supplemented with 10% FBS (complete DMEM) (Gibco, USA). Approximately 3 h prior to transfection, medium was replaced with 10 mL of fresh complete DMEM. At the time of transfection, the HEK293T cells were 70–90% confluent and were evenly distributed. For transfection study, pPAX2 plasmid (containing gag and pol genes) and pMD2 plasmid (containing vsv gene) were cotransfected with pLenti-GFP vector using calcium phosphate precipitation technique according to manufacturer's protocol (Invitrogen, USA). The transfection cocktail was slowly added to the HEK293T plated cells and plates were returned to the incubator for 16 h. Then medium was gently replaced with 10 mL of fresh complete DMEM. Virus-containing medium was harvested for 48 h and was centrifuged at 500 g for 10 min at 4°C and filtered through a 0.45 µm filter to remove debris and stored at 4°C accordingly. Transfection efficiency was determined using fluorescent microscopy described elsewhere.<sup>33</sup>

#### **Transduction and EGFP-labeling of iPSCs**

A 4 mL of virus-containing medium was added to 2 mL hiPSC media and gently poured into hiPSCs T25 flask. After 24 h of incubation, 70% of medium was replaced with fresh virus containing medium plus hiPSC media. In the next step, for selection of GFP labeled hiPSCs 2 µg mL<sup>-1</sup> puromycin was added to hiPSC media and was replaced with virus-containing media for the next 2 days. GFP labeled hiPSC colonies were detached with 0.1% collagenase IV and then transferred into nontreated six-well plates (Jet Biofil, Japan) for 3–5 days in embryoid body (EB) medium consisting of human hiPSC medium without human fibroblast growth factor 2 to form EB. GFP labeled embryoid bodies were observed with fluorescent microscopy.

#### **In vivo study**

**Utilization of transfected hiPSCs in animal models.** GFP labelled EBs were used to seed the hybrid microfluidic device as well as our control systems under identical conditions mentioned above. For all platforms, nearly 70% of medium was replaced every day. After 8 days of, the scaffolds in the microfluidic device were utilized in treatment of hemisectioned SCI rats as a group receiving cell containing scaffold. To have control, a group of animals received differentiated cells in suspension form, which were obtained from microfluidic device (i.e., they were detached using collagenase IV).

**Surgical procedure and animal care.** Animal procedure has been conducted under the approval of animal care and use committee of Tehran University of Medical Sciences. Female Wistar rats (Tehran University Animal Laboratory) weighing 200–250 g were deeply anesthetized with IP injection of ketamine 50 mg kg<sup>-1</sup> (Fort Dodge Animal Health, Fort Dodge, IA) and xylazine 5 mg kg<sup>-1</sup> (Lloyd Laboratories, Shenandoah, IA). Animals were placed on a heating pad

constantly maintained at 37°C during surgery, backs were shaved and aseptically prepared. A 5-cm incision was made along the dorsal midline. Multiple laminectomies were performed with sharp scissors at levels T8–T10 while ensuring that the facet joints were not violated. The posterior aspect of the spinal cord was exposed. An angled micro-scissor was used for a lateral hemisection of the spinal cord at level T9, outlying a triangle segment of spinal cord, approximately less than 1.0 mm<sup>2</sup>. The surgical procedure was performed under stereo microscope (Zeiss stemi 2000, Germany).

Animals were divided into following groups: (1) Group #1 receiving differentiated cells embedded in scaffold ( $n = 13$ ), (2) Group #2 receiving differentiated cells detached from scaffolds in the form of cell suspension ( $n = 8$ ), and (3) group #3 receiving no cells with just empty lesions (control group) ( $n = 9$ ). In the first group, biodegradable PLGA scaffolds containing neural differentiated hiPSCs were placed on the cavity, making sure that the severed ends of the cord were covered completely. Second group received cell suspension and attempts were made to slowly inject cells exactly in the formed cavity, in a total volume of 10  $\mu\text{L}$  ( $\sim 250,000$  cells). Control animals received no implants. Exposed spinal cords in three groups were covered with muscles and fascia. Muscle layers and skin were sutured and animals recovered in clean, low-sided cages to ensure easy access to food and water. Bladders were evacuated twice daily until reflex bladder function was established.

Gentamicin (12 mg kg<sup>-1</sup>) and cefazolin (50 mg kg<sup>-1</sup>) were given IP for 2 weeks to prevent infection. Dexamethasone 0.3–0.6 mg kg<sup>-1</sup> was also administered to reduce inflammatory reactions and its immunosuppression effect was also considered. All animals survived for 1 month. The surgeries for the implant plus controls were performed at the same time to minimize differences between groups arising from any refinement in surgical technique during the study. Hemisections were alternated between the right and left sides to further reduce bias.

**Functional recovery and behavioral studies.** On days 1, 7, 14, and 28 post injury, behavioral analysis was performed by two observers blinded to the treatments. Rats were allowed to move freely in a 1 m<sup>2</sup> box with a black surface and were scored during 4 min for their ability to use their hindlimbs. Joint movements, paw placement, weight support, and fore/hindlimb coordination were judged according to the 21-point BBB locomotion scale. The BBB-test was used to distinguish between movements of individual components of the hind limb. The test was video recorded for later analysis.

**Tissue preparation and freeze section.** Animals in group 1 (cell containing scaffold) and group 2 (cell suspension) were sacrificed at 1, 2 and 4 weeks after surgery. Animals were deeply anesthetized with ketamin 60 mg kg<sup>-1</sup>, xylazine 5 mg kg<sup>-1</sup>. Following perfusion, spinal cords were carefully dissected, post-fixed overnight in 4% paraformal-

dehyde in 4°C and dehydrated serially in 10% and 30% sucrose overnight at 4°C. One centimeter blocks of the cords including injury epicenters were embedded in OCT and cryo-sectioned with Sakura, Tissue-Tek, cryo3 (Japan) in 4- $\mu\text{m}$ -thick sections. Because of GFP-label of grafted hiPSCs, slide staining was not necessary for detection of differentiated stem cells. Grafted cells were easily followed utilizing fluorescent microscopy (Nikon, Japan).

### Statistical analysis

The acquired data of qPCR were analyzed by REST 2009.  $p$  values  $< 0.05$  were considered as statistically significant. Asterisk (\*) shows that the result is significant  $p \leq 0.001$ . Each experiment was repeated independently at least three times. In functional behavior scoring, Shapiro–Wilk test was used to determine the normality (Gaussian-shaped distribution) of the data. The BBB data showed significant departure from a normal distribution for all time points beyond day 28. For day 28 parametric methods were used including repeated measures analysis of variance (ANOVA) and Holm–Sidak *post hoc* analysis for multiple group comparisons to determine the statistical significance of the results. The inclined plane data showed a significant departure from a normal distribution and was analyzed with the Kruskal–Wallis  $H$  test, followed by the Dunn’s test to identify specific group differences when the Kruskal–Wallis test showed significance ( $p < 0.05$ ).

## RESULTS

### Characterization of cells inside the microfluidic system

The hybrid microfluidic chip and operational scheme are illustrated in Figure 1(b,c). The designed two-layer microfluidic device was composed of a microchannel network integrated with 32 cell culture chambers bonded to a PLGA coated substrate. The device was fabricated by using soft lithography technique, in which the top layer was PDMS, and the bottom layer was a glass substrate coated with nanofibers of PLGA. The 32 cell culture chambers had identical sizes with 5 mm in length and 0.07 mm in width with a shared inlet and outlet. To fabricate PLGA nanofibers, an electrospinning technique was used with aforementioned details. Electrospinning of PLGA-based nanofibers resulted in a scaffold composed of porous, bead free, uniform, aligned fibers with average diameter of 100–200 nm, as observed by SEM [Fig. 2(a)]. Fluorescent images of hiPSCs on nanofiber scaffolds are shown on Figure 2(d). Detailed morphology of hiPSCs colonies on nanofiber scaffolds are also shown in Figure 2(b). The overall results indicate that the hiPSCs were well attached on the scaffolds and the original round shape cells show new dendritic spines in day 8 in order to differentiate into neurons Figure 2(c).

ATR-FTIR spectroscopy was performed to confirm the grafting of fibronectin peptide onto the surface of PLGA nanofibers. As can be seen in Supporting Information Figure S1, there are three new sharp peaks on about 1600 which reveal fibronectin amide bonds and one broad peak is observable around 3500 that seems to relate to N–H bonds of fibronectin amino-acids. Biocompatibility of the scaffolds

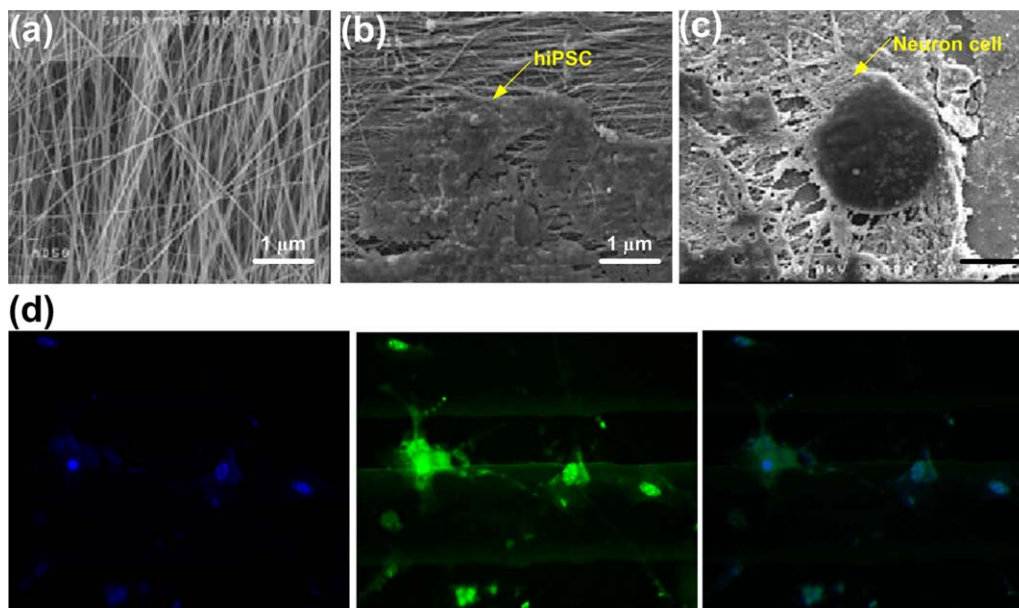


**FIGURE 2.** (a) SEM micrographs of PLGA nanofibrous scaffolds with aligned and uniform fibers and average diameter of 100–200 nm. (b) hiPSCs colonies attachment on aligned of PLGA nanofibers (c) SEM image of a round shape cell showing formation of new dendritic spines in order to differentiate into neurons with 8 days. (d) Florescent image of differentiated hiPSCs with the dendritic spines inside the microfluidic device after 8 days. Neural marker of NSE was utilized with DAPI co-staining.

was investigated via MTT assay, which revealed the significant viability and proliferation rate of hiPSCs on both types of nanofibrous scaffold but with higher values for fibronectin treated PLGA compared to plasma treated one (see Supporting Information Fig. S2;  $p < 0.05$ )

#### Quantitative real-time RT-PCR

The expression of neural genes was examined in hiPSCs in order to confirm neural differentiation after culturing cells on four different conditions (i.e., TCPS, PLGA scaffold with and without neurotrophic factors and hybrid microfluidic system) by induction reagents supplemented with growth factor. The results related to the expression of five genes among the differentiated cells are depicted in Figure 3. After culturing cells in four different conditions, mRNA levels encoding for BDNF, MAP-2, NSE,  $\beta$ -tubulin III and glial lineage marker (GFAP) were higher compared to undifferentiated hiPSCs cultured on TCPS without induction media, confirming neuronal differentiation of these cells. Analysis of results revealed that BDNF and NSE expression levels were not significantly different in various conditions. However, expression of MAP2 and GFAP genes in the microfluidic device were considerably less than other conditions. As GFAP is a classic marker for astrocytes (star-shaped glial cells in the brain and spinal cord) – i.e., during neuronal differentiation expression of GFAP should be decreased- therefore, microfluidic device is turned to be more suitable for neuronal differentiation in comparison to other culture conditions.  $\beta$ -tubulin III is one of the most important neuronal-related genes and qPCR results demonstrated elevated expression of their mRNA in comparison to other surfaces. Hence, our hybrid microfluidic device showed the optimum characteristics for differentiation of hiPSCs into neurons evi-

dence by elevated expression of the  $\beta$ -tubulin III and reduction of GFAP expression level.

#### Immunocytochemistry analysis

Immunocytochemistry was performed to investigate the cellular localization of neuronal markers after 8 days of differentiation in the microfluidic device. Expression of the transcription factors including  $\beta$ -tubulin III and NSE proteins was assessed by immunofluorescent staining which confirmed their presence in hiPSCs differentiated in all surfaces. Anti  $\beta$ -tubulin III and anti NSE antibodies reflect the green light under fluorescent microscopy and cell's

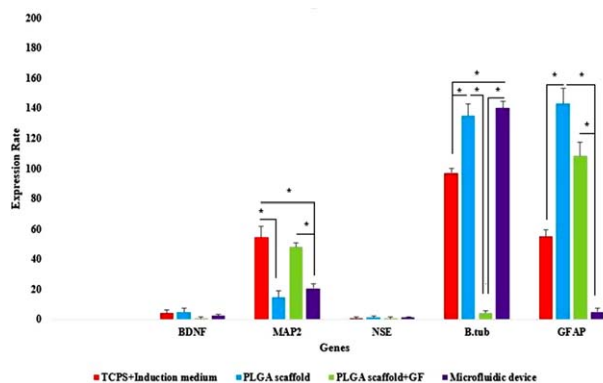


**FIGURE 3.** Neural gene expressions in differentiated hiPSCs on different induction surfaces. The cells were maintained in four different induction systems for 8 days and analyzed for expression of neuronal genes. The column ratio of mRNA expression levels is the expression rate of genes compared with untreated cells. Beta-actin was used as a control for RNA sample quality. REST software was used for gene expression analyses using real-time PCR data from the rotor-gene Q. Results are presented as mean  $\pm$  SD. Significant levels are  $*p \leq 0.05$ .

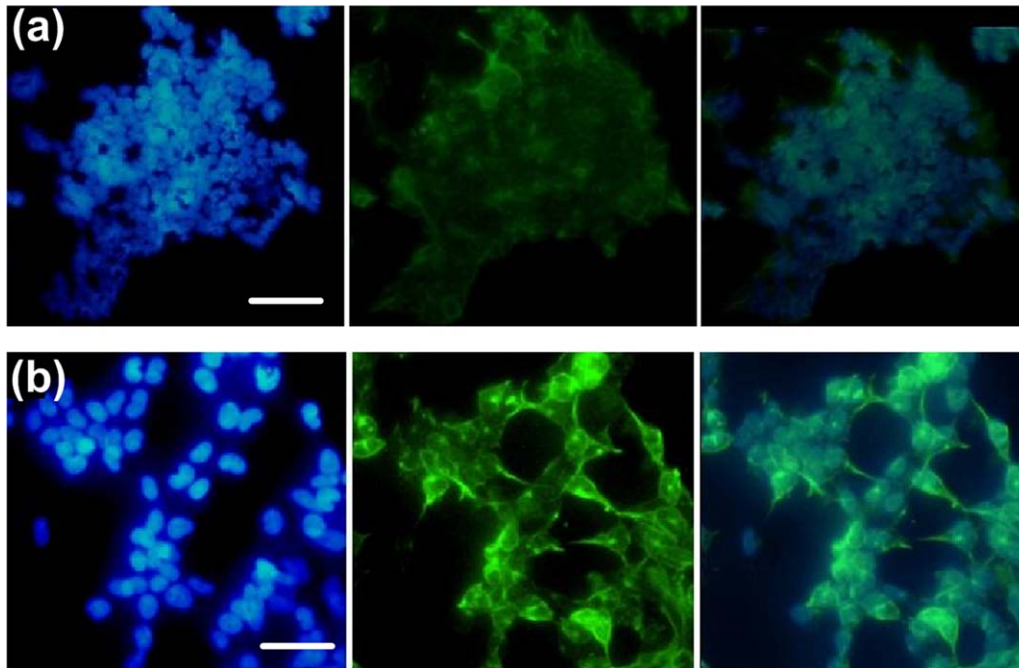


**FIGURE 4.** The cells were subjected to immunocytochemistry analysis for the expression of neural markers including  $\beta$ -tubulin III (green). Cells were co-stained with DAPI to visualize nuclei (blue). (a) Immunocytochemistry of undifferentiated hiPSCs in day 8. (b) Immunocytochemistry of neural differentiated hiPSCs in hybrid microfluidic system in day 8.

nucleus was co-stained with 4,6-diamidino-2-phenylindole (DAPI) to be visible with blue color. Control cells do not show dendritic spines and express green color in lower strength [Fig. 4(a)] while in microfluidic device, the green color (presence of neural markers) is expressed with higher strength and dendritic spines are clearly observable in  $\beta$ -tubulin III [Fig. 4(b)] and in NSE [Fig. 2(d)].

#### EGFP labeling of hiPSCs

Fluorescent microscopy imaging revealed that GFP expressing gene was incorporated in hiPSC's genome and all the transduced and selected cells express a bright green color under 509 nm wavelength. On the other hand, because EGFP is a red shifted GFP, it also emits red color when illuminated with green light. Therefore, labeled cells [Supporting Information Fig. S3(a)] are able to express both green [Supporting Information Fig. S3(b)] and red light [Supporting Information Fig. S3(c)] under fluorescent microscope using different filters.

#### *In vivo* study

**Behavioral and functional analysis.** Recovery of locomotor function was assessed using the BBB rating scale. No significant difference in BBB scores was observed between three groups on days 1 and 7, while behavioral study showed a significant decrease in locomotor function in the groups receiving cell suspension versus control and those having cell containing scaffold. However, group having cell containing scaffold showed better function on day 28 in comparison with control group; the difference was not statistically significant (see Supporting Information Fig. S4).

#### Characterization of grafted cells after delivery to hemisected cord

Animals were sacrificed 1, 2, and 4 weeks post transplantation and their spinal cords were harvested for histology study. Fluorescent microscopy analysis revealed that in the group that just received cell suspension, population of differentiated hiPSCs was decreased from the first week to the fourth week. It is probably due to lack of cell resistance in injury site and diffusion of cells to adjacent tissues over time (Fig. 5). In the group that received cell with scaffolds, despite receiving approximately equal number of cells to the group receiving cell suspension, the number and concentration of hiPSCs were increased over time (Fig. 6). It seems that this significant difference between two groups relates to the matrix-mediated signals (i.e., obtained by engrafting cells into polymeric scaffolds), showing more profound impact on hiPSCs phenotypes and functionality.

#### DISCUSSION

The capacity of regeneration in central nervous system (CNS) still remains a complicated issue. Previous studies have demonstrated that controlling stem cells fate is strongly directed by cell-to-cell and cell-to-extracellular matrix (ECM) interaction.<sup>34,35</sup> Thanks to advances in microfluidic technologies, we are beginning to systematically investigate the response of cells to combinations of relevant mechanobiological stimuli under well-controlled microenvironments.<sup>36</sup> Although hiPSCs have been studied extensively using bench-top systems, a detailed understanding of their behavior in *in vivo*-like microenvironments which promote their differentiation is still lacking.

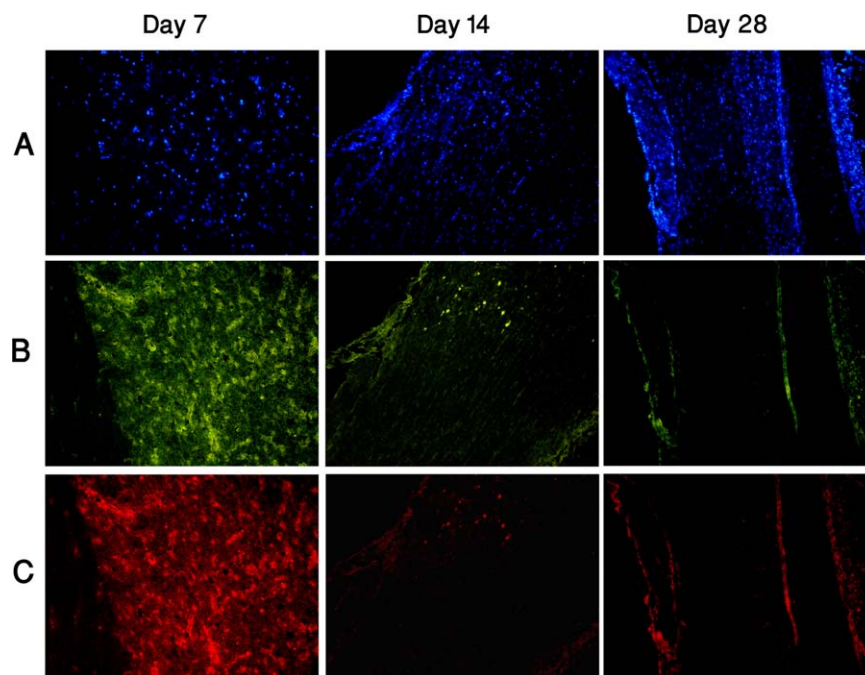


**FIGURE 5.** Injected cells survival in hemisected rat spinal cord after surgery during 28 days of animal study in group receiving cell suspension. (A) DAPI stained nuclei. (B) GFP-labeled differentiated hiPSCs which were injected to rat injured spinal cord. (C) The same cells as second row with their red emission.

Most cells are in contact with ECMs and various studies have shown ECM can induce specific signaling pathways among its several functions to direct stem cell fate. In this regard, numerous strategies such as micro-patterning, protein immobilization and utilization of 3D scaffolds have presented unique insights into the role of ECM based signaling for neural differentiation and cell guidance.<sup>24</sup> The cell guidance has been used to investigate cell behavior in the treatment of spinal cord injury and neurodegenerative diseases of the CNS.<sup>37–39</sup>

*In vivo* microenvironment is complex and can exert multiple cues on cells, consisting of combinatorial stimuli of biochemical, biomechanical, and/or biophysical nature.<sup>40</sup> In this study, we decided to build a niche microenvironment for effective differentiation of hiPSCs into neuron cells for utilization in spinal cord injuries. Our main goal was to provide necessary physical and chemical factors for cell stimulation using a hybrid culture device. Compared with 2D culture systems, our microfluidic device help these cells grow in 3D microenvironments more similarly to their *in vivo* phenotypes, thus promoting cell–cell and cell–matrix interactions. The incorporated nanofibers are capable of encapsulating cells, and have shown to be more useful for tissue engineering.<sup>41</sup> Given the significant influence of ECM proteins (e.g., collagen, laminin, fibronectin) on cellular functions, we have coated our PLGA scaffold with fibronectin to promote neuroprotective differentiation of hiPSCs as shown by other researchers.<sup>42</sup> Eventually, utilization of fluidic networks on these scaffolds enabled us to integrate the chemical and physical perturbations with relative ease in a confined microenvironment, which leads to a much greater analysis throughput that requires smaller amounts of reagents.

Systematic study of cellular behavior revealed that the microenvironment produced by the hybrid microfluidic system can enhance and diminish the expression of some neuronal genes. In particular, the differentiated cells inside the microfluidic device expressed higher level of  $\beta$ -tubulin III neural genes while GFAP<sup>30</sup> genes were expressed at lower levels compared to other three conditions (i.e., PLGA scaffold with and without growth factors and TCPS dishes). Taken together, these results suggest that hiPSCs differentiated inside microfluidic devices are more likely to differentiate toward neural cells, while other condition mainly promote differentiation into glial cells. We believe this can be attributed to the immobilized biochemical factors synergized with aligned nanofibers in a restrict microenvironment which promotes efficient induction of hiPSCs.

Maintenance of cellular microenvironment for tissue engineering is another important finding of our study. *In vivo* engraftment of differentiated cells (i.e., with and without scaffold) obtained from microfluidic system revealed the crucial role of ECM on cell spreading which could determine the cellular decision to undergo apoptosis or cell growth.<sup>43</sup> Proliferation of cells embedded in scaffolds (Fig. 6) inside the animal models indicate that ECM modulate cellular phenotypes by acting as a glue that holds cells together and by presenting biological cues in different shapes, topography, and as direct mechanical forces.<sup>44</sup>

On the other hand, long-term monitoring of functional behavior of the rats during 7, 14, and 28 days post transplantation revealed no significant improvement among all groups. One possible reason can be inadequate formation of synapses between hiPSC-derived neurons and host mouse spinal cord neurons. Although previous studies have shown better

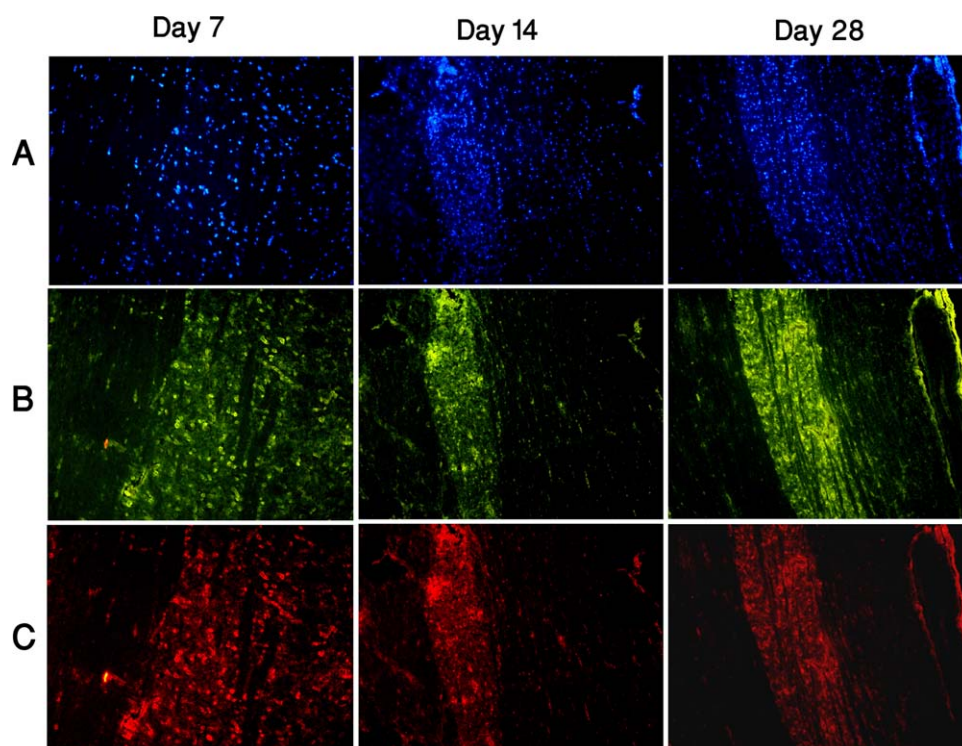


**FIGURE 6.** Scaffold loaded cells survival in hemisectioned rat spinal cord after surgery during 28 days of animal study in cell containing scaffold group. (A) DAPI stained nuclei. (B) GFP-labeled differentiated scaffold loaded hiPSCs which were implanted in rat injured spinal cord. (C) The same cells as second row with their red emission.

functional recovery in transplanting hiPSC-derived neurospheres (hiPSC-NSs) into SCID mice,<sup>45</sup> the intriguing work of Nutt SE et al. demonstrated that integration of hiPSC-derived neural cells in the early chronic cervical model did not lead to significant improvement in forelimb functionality, which is in good agreement with our findings.<sup>46</sup> Taken together, the results of these studies suggest that although utility of hiPSCs show great promise for cellular therapy, future studies should focus on the specific hiPSC-derivatives or cotherapies that will restore function in the SCI.

## CONCLUSIONS

Recent advancement in microfluidics and tissue engineering has allowed researchers to unveil many aspects of bio-chemical/mechanical regulation, especially in the context of stem cells. Miniaturized microfluidic platforms offer stem cells an *in vivo*-like microenvironment that is challenging to be realized in conventional benchtop systems. In this study, we developed a hybrid microfluidic system to make a suitable micro-environment for differentiation of hiPSCs into neuron cells under controlled conditions. Although utilization of nanofibrous scaffolds are shown to be useful in tissue engineering,<sup>47</sup> the results of this study demonstrated that integration of fluidic channels can enhance the differentiation process, that is, by confining the soluble factors within environments of cultured cells and facilitating the cross-talk between adjacent cells. This platform can be served also as a good starting point for future studies regarding the use of

topographical cues to enhance central nervous system regeneration. This platform offers several advantages compared to traditional *in vitro* methods used to engineer neural cells for regenerative medicine. First, our system allows us to perform perfusion with the infusion of assay reagents while the optical transparency gives us the flexibility to do real-time imaging and analysis of the cellular response. Second, the developed microfluidic-based platform can reduce the amount of cells and reagents and consequently decrease the costs compared to conventional techniques. Cultured cells in this system can discern the physical and chemical cues from the substrate at micro/nanometer scales thus helping them to initiate the expression of specific genes or signaling pathways for differentiation. Finally, our device prepares oriented cell on biocompatible and biodegradable scaffolds with high yield, which is suitable for tissue engineering applications.

## REFERENCES

1. Lai BQ, Wang JM, Ling EA, Wu JL, Zeng YS. Graft of a tissue-engineered neural scaffold serves as a promising strategy to restore myelination after rat spinal cord transection. *Stem Cells Dev* 2013;23:910–921.
2. Anderson KD, Sharp KG, Steward O. Bilateral cervical contusion spinal cord injury in rats. *Exp Neurol* 2009;220:9–22.
3. Zamani F, Amani-Tehran M, Latifi M, Shokrgozar MA, Zaminy A. Promotion of spinal cord axon regeneration by 3D nanofibrous core-sheath scaffolds. *J Biomed Mater Res Part A* 2014;102A:506–513.
4. Segers VFM, Lee RT. Stem-cell therapy for cardiac disease. *Nature* 2008;451:937–942.
5. Raasch K, Malecki E, Siemann M, Martinez MM, Heinisch JJ, Bakota J, Kaltschmidt C, Kaltschmidt B, Rosmeyer H, Brandt R.

- Identification of nucleoside analogs as inducers of neuronal differentiation in a human reporter cell line and adult stem cells. *Chem Biol Drug Design* 2015;86. PUB-ID: 2713693
6. Temple S. The development of neural stem cells. *Nature* 2001; 414:112–117.
  7. Gage FH. Mammalian neural stem cells. *Science* 2000;287:1433–1438.
  8. Nadri S, Kazemi B, Eslaminejad MB, Yazdani S, Soleimani M. High yield of cells committed to the photoreceptor-like cells from conjunctiva mesenchymal stem cells on nanofibrous scaffolds. *Mol Biol Rep* 2013;40:3883–3890.
  9. Takahashi K, Tanabe K, Ohnuki M, Narita M, Ichisaka T, Tomoda K, Yamanaka S. Induction of pluripotent stem cells from adult human fibroblasts by defined factors. *Cell* 2007;131:861–872.
  10. Park IH, Zhao R, West JA, Yabuuchi A, Huo H, Ince TA, Lerou PH, Lensch MW, Daley GQ. Reprogramming of human somatic cells to pluripotency with defined factors. *Nature* 2008;451:141–146.
  11. Lowry WE, Richter L, Yachechko R, Pyle AD, Tchieu J, Sridharan R, Clark AT, Plath K. Generation of human induced pluripotent stem cells from dermal fibroblasts. *Proc Natl Acad Sci USA* 2008; 105:2883–2888.
  12. Okada M, Oka M, Yoneda Y. Effective culture conditions for the induction of pluripotent stem cells. *Biochim Biophys Acta* 2010; 1800:956–963.
  13. Mahairaki V, Ryu J, Peters A, Chang Q, Li T, Park TS, BurrIDGE PW, Talbot CC, Asnaghi L, Martin LJ, Zambidis ET, Koliatsos VE. Induced pluripotent stem cells from familial Alzheimer's disease patients differentiate into mature neurons with amyloidogenic properties. *Stem Cells Dev* 2014;23:2996–3010.
  14. Hanna J, Wernig M, Markoulaki S, Sun CW, Meissner A, Cassady JP, Beard C, Brambrink T, Wu LC, Townes TM, Jaenisch R. Treatment of sickle cell anemia mouse model with iPS cells generated from autologous skin. *Science* 2007;318:1920–1923.
  15. Xu CY, Inai R, Kotaki M, Ramakrishna S. Aligned biodegradable nanofibrous structure: A potential scaffold for blood vessel engineering. *Biomaterials* 2004;25:877–886.
  16. Bilousova G, Jun du H, King KB, De Langhe S, Chick WS, Torchia EC, Chow KS, Klemm DJ, Roop DR, Majka SM. Osteoblasts derived from induced pluripotent stem cells form calcified structures in scaffolds both in vitro and in vivo. *Stem Cells* 2011;29: 206–216.
  17. Nelson T, Martinez-Fernandez A, Yamada S, Perez-Terzic C, Ikeda Y, Terzic A. Repair of acute myocardial infarction by human stemness factors induced pluripotent stem cells. *Circulation* 2009;120: 408–416.
  18. Wernig M, Zhao JP, Pruszak J, Hedlund E, Fu D, Soldner F, Broccoli V, Constantine-Paton M, Isacson O, Jaenisch R. Neurons derived from reprogrammed fibroblasts functionally integrate into the fetal brain and improve symptoms of rats with Parkinson's disease. *Proc Natl Acad Sci USA* 2008;105:5856–5861.
  19. Zhang N, An MC, Montoro D, Ellerby LM. Characterization of human Huntington's disease cell model from induced pluripotent stem cells. *PLoS Curr* 2010;2:RRN1193.
  20. Song B, Sun G, Herszfeld D, Sylvain A, Campanale NV, Hirst CE, Caine S, Parkinson HC, Tonta MA, Coleman HA, Short M, Ricardo SD, Reubinoff B, Bernard CC. Neural differentiation of patient specific iPS cells as a novel approach to study the pathophysiology of multiple sclerosis. *Stem Cell Res* 2012;8:259–273.
  21. Tsuji O, Miura K, Okada Y, Fujiyoshi K, Mukaino M, Nagoshi N, Kitamura K, Kumagai G, Nishino M, Tomisato S, Higashi H, Nagai T, Katoh H, Kohda K, Matsuzaki Y, Yuzaki M, Ikeda E, Toyama Y, Nakamura M, Yamanaka S, Okano H. Therapeutic potential of appropriately evaluated safe-induced pluripotent stem cells for spinal cord injury. *Proc Natl Acad Sci USA* 2010;107:12704–12709.
  22. Wang Y, Lee WC, Manga KK, Ang PK, Lu J, Liu YP, Lim CT, Loh KP. Fluorinated graphene for promoting neuro-induction of stem cells. *Adv Mater* 2012;24:4285–4290.
  23. Zhang J, Li L. Stem cell niche: Microenvironment and beyond. *J Biol Chem* 2008;283:9499–9503.
  24. Kshitiz, Park J, Kim P, Helen W, Engler AJ, Levchenko A, Kim DH. Control of stem cell fate and function by engineering physical microenvironments. *Integr Biol* 2012;4:1008–1018.
  25. Warkiani EM, Lim CT. *Microfluidic Platforms for Human Disease Cell Mechanics Studies*. Materiomics: Multiscale Mechanics of Biological Materials and Structures. Springer Vienna 2013; 107–119.
  26. Conover JC, Notti RQ. The neural stem cell niche. *Cell Tissue Res* 2008;331:211–224.
  27. Polacheck WJ, Li R, Uzel SGM, Kamm RD. Microfluidic platforms for mechanobiology. *Lab Chip* 2013;13:2252–2267.
  28. Chaudhuri PK, Warkiani ME, Jing T, Lim CT. Microfluidics for research and applications in oncology. *Analyst* 2016;141:504–524.
  29. Shemesh J, Jalilian I, Shi A, Yeoh GH, Knothe Tate ML, Warkiani ME. Flow-induced stress on adherent cells in microfluidic devices. *Lab Chip* 2015;15:4114–4127.
  30. Eglitis MA, Mezey E. Hematopoietic cells differentiate into both microglia and macroglia in the brains of adult mice. *Proc Natl Acad Sci USA* 1997;94:4080–4085.
  31. Warkiani ME, Lou CP, Liu HB, Gong HQ. A high-flux isopore micro-fabricated membrane for effective concentration and recovering of waterborne pathogens. *Biomed Microdev* 2012;14:669–677.
  32. Ardeshiryajimi A, Soleimani M, Hosseinkhani S, Parivar K, Yaghmaei P. A comparative study of osteogenic differentiation human induced pluripotent stem cells and adipose tissue derived mesenchymal stem cells. *Cell J* 2014;16:235–244.
  33. Taniyama Y, Tachibana K, Hiraoka K, Aoki M, Yamamoto S, Matsumoto K, Nakamura T, Ogihara T, Kaneda Y, Morishita R. Development of safe and efficient novel nonviral gene transfer using ultrasound: Enhancement of transfection efficiency of naked plasmid DNA in skeletal muscle. *Gene Ther* 2002;9:372–380.
  34. Doetsch F. A niche for adult neural stem cells. *Curr Opin Genet Dev* 2003;13:543–550.
  35. Panchision DM, McKay RD. The control of neural stem cells by morphogenic signals. *Curr Opin Genet Dev* 2002;12:478–487.
  36. Wilson CJ, Clegg RE, Leavesley DI, Percy MJ. Mediation of biomaterial-cell interactions by adsorbed proteins: A review. *Tissue Eng* 2005;11:1–18.
  37. Bunge MB. Bridging areas of injury in the spinal cord. *Neuroscientist* 2001;7:325–339.
  38. Hayman MW, Smith KH, Cameron NR, Przyborski SA. Growth of human stem cell-derived neurons on solid three-dimensional polymers. *J Biochem Biophys Methods* 2005;62:231–240.
  39. Teng YD, Lavik EB, Qu X, Park KI, Ourednik J, Zurakowski D, Langer R, Snyder EY. Functional recovery following traumatic spinal cord injury mediated by a unique polymer scaffold seeded with neural stem cells. *Proc Natl Acad Sci USA* 2002;99:3024–3029.
  40. Yamada KM, Cukierman E. Modeling tissue morphogenesis and cancer in 3D. *Cell* 2007;130:601–610.
  41. Kim DH, Beebe DJ, Levchenko A. Micro- and nanoengineering for stem cell biology: The promise with a caution. *Trends Biotechnol* 2011;29:399–408.
  42. Ding T, Lu WW, Zheng Y, Li Zy, Pan Hb, Luo Z. Rapid repair of rat sciatic nerve injury using a nanosilver-embedded collagen scaffold coated with laminin and fibronectin. *Regen Med* 2011;6:437–447.
  43. Chen CS, Mrksich M, Huang S, Whitesides GM, Ingber DE. Geometric control of cell life and death. *Science* 1997;276:1425–1428.
  44. Patel S, Kurpinski K, Quigley RJ, Gao H, Hsiao BS, Poo MM. Bioactive nanofibers: Synergistic effects of nanotopography and chemical signaling on cell guidance. *Nano Lett* 2007;7:2122–2128.
  45. Nori S, Okada Y, Yasudaa A, Tsuji O, Takahashia Y, Kobayashia Y, Fujiyoshib K, Koiked M, Uchiyamada Y, Ikeda E, Toyama Y, Yamanakag S, Nakamurab M, Okano H. Grafted human-induced pluripotent stem-cell-derived neurospheres promote motor functional recovery after spinal cord injury in mice. *Proc Natl Acad Sci USA* 2011;108:16825–16830.
  46. Nutt SE, Chang EA, Suhr ST, Schlosser LO, Mondello SE, Moritz CT, Cibelli JB, Horner PJ. Caudalized human iPSC-derived neural progenitor cells produce neurons and glia but fail to restore function in an early chronic spinal cord injury model. *Exp Neurol* 2013;248:491–503.
  47. Li X, Xiao Z, Han J, Chen L, Xiao H, Ma F, Hou X, Li X, Sun J, Ding W, Zhao Y, Chen B, Dai J. Promotion of neuronal differentiation of neural progenitor cells by using EGFR antibody functionalized collagen scaffolds for spinal cord injury repair. *Biomaterials* 2013;34:5107–5116.